Measuring noninertial physics of turbulence: Quasiscaling analysis

Jian-Zhou Zhu
State Key Laboratory for Turbulence and Complex Systems and Department of Mechanics and Engineering Science, Peking University, Beijing 100871, People's Republic of China

(Received 30 January 2005; revised manuscript received 9 May 2005; published 18 August 2005)

Quasiscaling exponent $\zeta_n^{M;D}$ is introduced by the ratio of turbulence velocity structure functions $S_n(r^D)/S_n(r^M)=(r^D/r^M)^{\zeta_n^{M;D}}$ at scales r^M and r^D to measure the viscous and large-scale effects. Two inertial phenomenologies, respectively, that by She and Leveque [Phys. Rev. Lett. **72**, 336 (1994)] and that by Meneveau and Sreenivason [Phys. Rev. Lett. **59**, 1424 (1987)], are extended for quasiscaling as case studies. Both extended models fit well to the measurements and quantify the noninertial behaviors from different physical aspects, i.e., logarithmic-nonhomogeneous Poissonian and nonconservative binomial cascade, through the scale-dependent behaviors of the model parameters extracted from experimental data; and the physical meanings of the extended self-similarity properties for them are exposed.

DOI: 10.1103/PhysRevE.72.026303 PACS number(s): 47.27.Gs, 47.53.+n, 05.45.Tp, 47.27.Jv

I. INTRODUCTION

Inertial physics of turbulence has long been attacked [1]; however Kraichnan cautioned [2]

> "The Kolmogorov theories have profoundly shaped and illuminated thinking about turbulence. But, in one respect, this influence perhaps has been unfortunate: relatively little attention has been devoted to the prediction of turbulence statistics at finite Reynolds numbers. Finite Reynolds number turbulence has a rich and interesting structure. Moreover, it is likely that the questions of intermittency correction to K41 can be resolved only when a detailed understanding of dynamics at finite Reynolds numbers has been achieved."

Noninertial physics of turbulence concerns the viscous and large-scale effects embodied in the bendings in the log-log plot of statistical moments, such as velocity structure functions, versus scales or Fourier spectrum versus wave numbers (or frequencies) among others [3]. Following the idea of gradual viscous cutoff [4], scale-dependent singularity exponent and the concept of multifractal universality have been introduced [1] to account for viscous effects. Recently, especially inspired by the observation of extended self-similarity (ESS) [5], Batchelor-type parametrizations, originally used as a simple transition function from inertial to viscous range, regained employments, even for the transition from inertial to large-scale stirring range [6] and, more courageously, for the transitions of the random multiplier and the probability distribution function (PDF) of the singularity exponent for Lagrangian velocity statistics [7]; and, very recently, analysis of turbulence under the framework of entropy introduced by Tsallis [8] has also received much interest [9]. Both approaches have won some successes, however dynamical understanding and physical justification are still lacking [10].

We will measure the curvatures in the log-log plot of velocity structure functions versus scales by the quasiscaling exponents. Physics of noninertial cascade is then revealed qualitatively by extending inertial phenomenology by She and Leveque (SL) [11] and that by Meneveau and Sreenivasan (MS) [12] to quasiscalings, quantifying viscous dissipating and external stirring effects. We manage to make inertial theories "fortunate" for the understanding of noninertial turbulence.

This paper is organized as follows. In Sec. II, we introduce the concept of quasiscaling and analyze an experimental turbulence by extending SL and MS models. Further approximation and analysis with ESS are made in Sec. III; and Sec. IV summarizes this work and offers further discussions.

II. QUASISCALING ANALYSIS

For the nth order velocity structure function $S_n(-\ln r) =\langle(\delta v_r)^n\rangle$, with δv_r being the velocity increment along the separation r and $\langle\cdot\rangle$ denoting the average, one can introduce a local scaling exponent, by taking the "time" $t=-\ln r$ and $L_n(t)=-\ln S_n(t)$ for convenience, with the form $\zeta_n^L(t) =dL_n(t)/dt$ (see, for example, Lohse *et al.* [6]). (Here and later, we use t or r depending on which one is more convenient in the situation.) We now define quasiscaling with mother- and daughter-eddy scales r^M and r^D,

$$S_n(t^D)/S_n(t^M) = (r^D/r^M)^{\zeta_n^{M;D}}, \tag{1}$$

and call $\zeta_n^{M;D}$ the quasiscaling exponent, which arises naturally from the random multiplicative process (RMP) model [1,11,12],

$$\delta v_{r^D} = W_{r^M r^D}\delta v_{r^M}, \tag{2}$$

with $\zeta_n^{M;D}=\ln\langle W^n_{r^M r^D}\rangle/\ln(r^D/r^M)$. Inertial scaling is a special scale-free case. It is evident that

$$\zeta_n^{M;D} = \int_{t^M}^{t^D} \zeta_n^L(t)dt/(t^D - t^M). \tag{3}$$

Concrete models are at hand by direct extensions of the inertial ones.

A. Logarithmic-nonhomogeneous Poissonian cascade

1. Extended SL phenomenology

In the RMP model, i.e., Eq. (2), if we take

$$P(W_{r^M r^D}) = e^{-\Lambda^{M;D}} \sum_{k=0}^{\infty} \frac{(\Lambda^{M;D})^k}{k!} \delta(W_{r^M r^D} - w_k^{M;D}) \tag{4}$$

with $w_k^{M;D} = e^{-\Gamma^{M;D}} \Pi_{i=0}^k \beta_i^{M;D}$ and let $\beta_i^{M;D} = \beta^{M;D}$ when $i \neq 0$ and $\beta_0^{M;D} = 1$, we have the quasiscaling exponent

$$^{\mathrm{SL}}\zeta_n^{M;D} = \gamma^{M;D} n + \lambda^{M;D}[1 - (\beta^{M;D})^n]; \tag{5}$$

and if further letting $\beta^{M;D} = \beta$, we obtain

$$^{\mathrm{SL}}\zeta_n^{M;D} = \gamma^{M;D} n + \lambda^{M;D}(1 - \beta^n) \tag{6}$$

and

$$^{\mathrm{SL}}\zeta_n^{L}(t) = \gamma(t) n + \lambda(t)(1 - \beta^n) \tag{7}$$

by Eq. (3): Here, a local rate function $\lambda(t)$ and the most singular exponent $\gamma(t)$ have been introduced by

$$\Lambda^{M;D} = \int_{t^M}^{t^D} \lambda(t) dt = \lambda^{M;D}(t^D - t^M) \tag{8}$$

and

$$\Gamma^{M;D} = \int_{t^M}^{t^D} \gamma(t) dt = \gamma^{M;D}(t^D - t^M). \tag{9}$$

The presuperscript "SL" comes from the fact that when $\gamma(t)$ and $\lambda(t)$ are constant, they reduce to the She-Leveque inertial scaling which was found able to be realized by logarithmic-Poisson statistics [11]. We now have the extended She-Leveque (ESL) quasiscaling by introducing the logarithmic-nonhomogeneous Poisson process (LNHPP) [13]. These results can also be obtained by direct extension of the hierarchical similarity (EHS) following the original derivation by She and Leveque [11] (see Sec. III A).

Poissonian statistics provides a quantized description of turbulent cascade (see She and Waymire [11]). The "energy" of the highest state of the cascade structure $W_{r^M r^D}$ is $w_0^{M;D} = (r^D/r^M)^{\gamma^{M;D}}$, and that of the intermediate state is $w_k^{M;D} = (r^D/r^M)^{\gamma^{M;D}} \Pi_{i=0}^k \beta_i^{M;D}$. When $\beta_i^{M;D} = \beta$, $\lambda(t)$, being constant in the inertial range, measures the arrival rate of the defect quanta β. More deep fluid dynamical and statistical meanings can be extrapolated from the thoughtful papers in Ref. [11]. Here, it is a simple scale-free to scale-dependent generalization. Similar ideas have in fact already been presented by Benzi *et al.* [14]. The equality $\beta_i^{M;D} = \beta$ $(i \neq 0)$ is, in fact, a requirement of the ESS property and can be tested by experiment (see text below and in Sec. III A); when ESS is not valid, Eq. (5) may still apply.

2. Measurement, fitting, and analysis

It is easy to measure the quasiscaling exponents (rather than the local scaling exponent, which concerns taking derivatives and is impossible for the discreteness of the data points which are especially sparse in the viscous range), and fit them with a certain model such as Eq. (6); and we call such a procedure quasiscaling analysis. We perform it in an experimental turbulent pipe flow studied previously in Refs. [15,16]. The objects are the time series of velocity signals at and along the center line of the pipe.

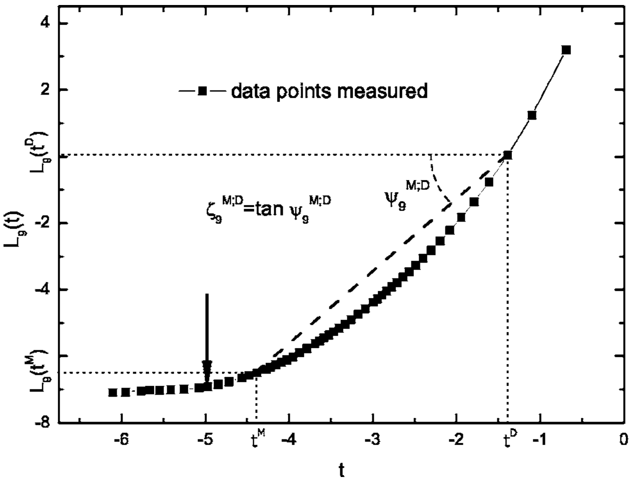

FIG. 1. The ninth order structure function, with the sketch of the quasiscaling exponent, measured at the center line of turbulent pipe flow. The arrow points to the largest mother-eddy scale $r_{\max}^{(M)} = 112$. The sketch shows that the quasiscaling exponent is $\zeta_n^{M;D} = \tan \Psi_n^{M;D}$, the slope of the slash connecting the two data points at mother- and daughter-eddy scales as denoted here for $n=9$.

Figure 1 is the plot for $L_9(t) = -\ln S_9(t)$ [17] and the sketch of the quasiscaling exponent, where the arrow points to the largest (mother-eddy) scale $r_{\max}^{(M)} = 112$ we will analyze, r being in units of sampling time applying Taylor's frozen flow assumption as in Refs. [15,16]. No inertial range appears and for scales much larger than $r_{\max}^{(M)}$ the structure function begins to saturate and we can observe that it varies with "time" t (or scale r) not in a monotonic way at some large-scale points subjecting to boundary effects or insufficient size of samples or others.

Figures 2 and 3 present, respectively, the excellent linear

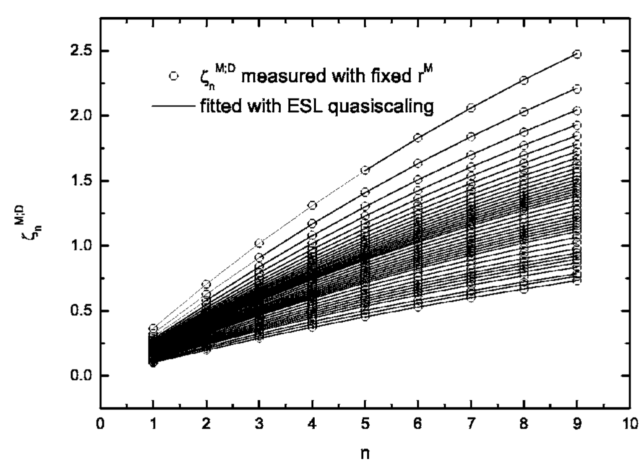

FIG. 2. $\zeta_n^{M;D}$ measured and fitted with ESL quasiscaling. Mother-eddy scale is fixed as $r^M = 112$. Larger exponents correspond to smaller daughter-eddy scale r^D ranging from 2 to 96.

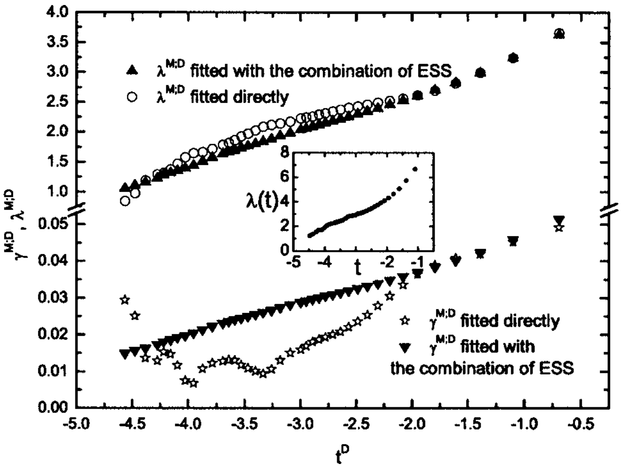

FIG. 3. Parameters fitted with SL quasiscaling directly, i.e., with Eq. (6) and with combination of ESS (see also Sec. III A). The inset presents the local rate function $\lambda(t)$ calculated by Eq. (8) from $\lambda^{M;D}$ fitted with the combination of ESS by central difference scheme.

least square fittings directly with Eq. (6) and the resulted parameters. In fact, we have done the nonlinear fitting with Eq. (5) and find that $\beta^{M;D}$ is nearly constant around 0.913 with very small variations and the improvements in fittings are unobservable with bare eyes, so we fix it; and we will show in Sec. III A that this is the requirement of the ESS property. We remark that fixing $r^M=112$ is for permitting a largest variation range of r^D and for convenience of calculation and one can also fix r^D and let r^M vary; and it should be noted that although the quasiscaling exponents and corresponding parameters depend on the choice of r^M and r^D, the local scaling exponents and corresponding parameters are invariable and so the fittings with ESL quasiscaling would be equally well for other choices of scales (such as those in EMS fitting in Sec. II B) as those presented here.

Figure 3 deserves further digestion. As commented in the end of Sec. II A 1, $\lambda(t)$ is the local defect rate of the cascade structure $W_{r^M r^D}$, measurement presented in this figure (observe the inset with its explanation in the caption and see the remark on physical model for it in Sec. IV) shows that it increases as "time" goes (r decreases), meaning dissipation accelerates the defect and so decelerates the energy cascade, i.e., decreases the energy transfer rate [1,19]. The variation law of $\gamma^{M;D}$ [or $\gamma(t)$] is similar to that of $\lambda^{M;D}$ [or $\lambda(t)$] (see also Sec. III A). Since $\gamma^{M;D}$ [or $\gamma(t)$] is the (local) exponent of the most intensive cascade structure $W^{(\infty)}_{r^M r^D}$ [or fluctuation $\delta v(t)^{(\infty)}$, $F_\infty(t)$ in Sec. III A], it is now indicated that viscosity weakens the cascade structures and gentles the fluctuations. External stirring acts on the opposite side. Following the SL phenomenology, codimension or probability interpretation [1,11] now tells that dissipation reduces the chance $(r^D/r^M)^{\lambda^{M,D}}$ to capture, with a ball of size r^D, the most intensive structures in a ball of size r^M; and the geometrical properties of the most intensive structures, which were claimed to be ideal vortex filaments in the inertial range of fluid turbulence by She and Leveque [11], vary with scale subjecting to dissipation and stirring effects, being continuously the intermediate objects between vortex globs [$\lambda(t)=0$], sheets [$\lambda(t)=1$], filaments [$\lambda(t)=2$], zero-dimension [$\lambda(t)=3$] and other minus-dimension structures [$\lambda(t)>3$], whose topologies change gradually as cascades proceed, the actual local codimension calculated by central difference from Eq. (8) is between 1 and 7 in the scale range analyzed as shown in the inset.

We conclude this section by remarking that when t^D (r^D) is near to t^M (r^M), the errors from moments in computing quasiscaling exponent become relatively evident for small $L_n(t^D)-L_n(t^M)$; and as $\gamma^{M;D}$'s are very small, contributing slightly to the exponents, their evaluations by direct fittings are sensitive to variations. The "anomalous" behavior for large r^D in Fig. 3 is understandable and can be largely eliminated by application of ESS property (see Sec. III A).

B. Nonconservative binomial cascade

1. Extended MS phenomenology

Meneveau and Sreenivasan have analyzed a simple binomial cascade model fitting well to the measured dimension spectrum [12]. The physical picture is simply that every mother-eddy breaks down into two equally sized daughter-eddies who inherit, respectively, $p^{M;D}$ and $q^{M;D}$ portion of the energy flux. It is direct to obtain extended Meneveau-Sreenivasan (EMS) quasiscaling,

$$ {}^{\mathrm{MS}}\zeta_n^{M;D} = 1 - \ln[(p^{M;D})^{n/3} + (q^{M;D})^{n/3}]/\ln(2) \qquad (10)$$

by taking $P(W_{r^M r^D})=(r^D/r^M)[\delta(W_{r^M r^D}-(p^{M;D})^{n/3})+\delta(W_{r^M r^D}-(q^{M;D})^{n/3})]$ in the RMP model, i.e., Eq. (2) or directly $P(\widetilde{W}_{r^M r^D})=(r^D/r^M)[\delta(\widetilde{W}_{r^M r^D}-p^{M;D})+\delta(\widetilde{W}_{r^M r^D}-q^{M;D})]$ in $\delta v_{r^D}^3=\widetilde{W}_{r^M r^D}\delta v_{r^M}^3$ with $r^M=2r^D$. Note that the energy flux F_r flowing through a domain of size r is estimated by $F_r\sim\delta v_r^3$ [1]. It is again a generalization from inertial cascade, where constant energy flux and degree of intermittency of energy transfer requires, respectively, $p^{M;D}+q^{M;D}=1$ and $p^{M;D}-q^{M;D}=0.4$ [12]; now dissipative extraction an external feeding breaks the conservation of energy flux and is quantified by $p^{M;D}+q^{M;D}-1$; and the degree of intermittency $p^{M;D}-q^{M;D}$ may also become scale dependent.

2. Measurement, fitting, and analysis

Figures 4 and 5 present the fittings of the measured quasiscaling exponent and the resulted parameters using the Levenberg-Marquardt nonlinear least square fitting algorithm with the help of software ORIGIN 7.0 for the same turbulence data used above. Fittings of the quasiscaling are satisfying though not so well as those by ESL after careful observation. Figure 5 shows that the total energy, denoted by $p^{M;D}+q^{M;D}$, inherited by corresponding daughter-eddies varies with scale and runs across the balance line $p^{M;D}+q^{M;D}=1$. Since no inertial range appears, turbulent fluctuations at all scales are subjected to mixing effects of viscous extraction and large-scale feeding; what we measured is the net result. Degree of intermittency is revealed by the difference between $p^{M;D}$ and $q^{M;D}$ and interestingly we find that the value $p^{M;D}-q^{M;D}\approx 0.4=0.7-0.3$ extends approximately over the noninertial range. We will verify in Sec. III B that this is a result of the ESS property.

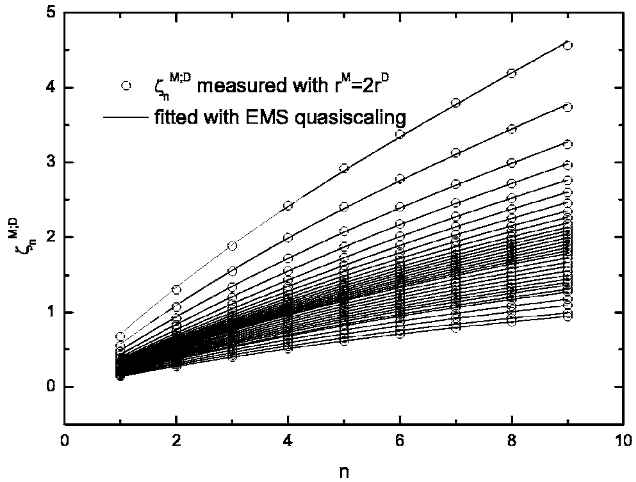

FIG. 4. $\zeta_n^{M;D}$ measured and fitted with EMS quasiscaling with $r^M=2r^D$. Larger exponents correspond to smaller scales with r^D ranging from 2 to 56.

III. FURTHER DIGESTION AND APPROXIMATION WITH ESS

Extended self-similarity claims the following relative scaling [5]:

$$S_n(t) \propto [S_3(t)]^{\zeta_n}. \tag{11}$$

It has been widely discussed and receives a blend of support and disapproval; for example, Meneveau [6] have shown that ESS is consistent with assuming the cutoff length decrease with increasing order of the moment but it is not always valid as shown by his multifractal formalism. We will verify by our measurements shown in the following sections that it is at least a very accurate approximation for moments of order not very high.

It is interesting to find that now we do not have to do the conventional linear fitting [5,15] in estimating the relative scaling exponent ζ_n. It is just the ratio of our quasiscaling exponents, i.e.,

$$\zeta_n = \zeta_n^{M;D}/\zeta_3^{M;D}. \tag{12}$$

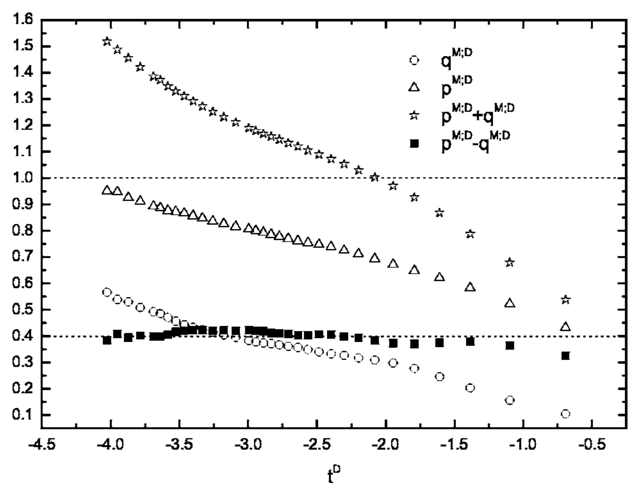

FIG. 5. Parameters fitted with MS quasiscaling. The two horizontal dashed lines designate, respectively, the balance line of dissipation and feeding ($p^{M;D}+q^{M;D}=1$) and the approximate degree of intermittency required by the ESS property (see Sec. III B).

A. ESS-ESL (EHS)

1. Formulation

We now extend the hierarchical similarity (EHS) of She and Leveque [11] as

$$\frac{F_{n+1}^{M;D}}{F_\infty^{M;D}} = \left(\frac{F_n^{M;D}}{F_\infty^{M;D}}\right)^{\beta^{M;D}}, \tag{13}$$

where

$$F_n^{M;D} = \frac{F_n(t^D) = S_{n+1}(t^D)/S_n(t^D)}{F_n(t^M) = S_{n+1}(t^M)/S_n(t^M)} = \frac{S_{n+1}(t^D)/S_{n+1}(t^M) = S_{n+1}^{M;D}}{S_n(t^D)/S_n(t^M) = S_n^{M;D}}.$$

From such an extension, it is easy to derive the ESL quasiscaling presented in Sec. II A 1; we do not pursue it here. Combining EHS and ESS, i.e., taking $F_\infty^{M;D}=(S_3^{M;D})^\Gamma$, and further letting $\beta^{M;D}=\beta$ to obtain the scale-free relative scaling exponents, we can rewrite Eq. (13) as

$$F_{n+1}^{M;D}/(S_3^{M;D})^\Gamma = [F_n^{M;D}/(S_3^{M;D})^\Gamma]^\beta. \tag{14}$$

Bring Eq. (11) into (14), we have the SL relative scaling exponent,

$$\zeta_n = \Gamma n + C(1-\beta^n), \tag{15}$$

which is constrained by $1=3\Gamma+C(1-\beta^3)$. Equation (6) together with Eqs. (12) and (15) leads to the following relations: $\lambda^{M;D}=C\zeta_3^{M;D}$, $\gamma^{M;D}=\Gamma\zeta_3^{M;D}$, and so $C/\Gamma=\lambda^{M;D}/\gamma^{M;D}=H$ or $\Gamma=\gamma^{M;D}=0$ (the so-called saturation of exponents when $n\to\infty$ [18]), i.e., λ is proportional to γ and this is why we remarked that the $\gamma^{M;D}$ directly fitted in Fig. 3 for large r^D is "anomalous."

We see that ESS-ESL (EHS) corresponds to take $P(W_{r^M r^D})=e^{-\Lambda^{M;D}}\Sigma_{k=0}^\infty[(\Lambda^{M;D})^k/k!]\delta[W_{r^M r^D}-(S_3^{M;D})^\Gamma\beta^k]$ in the RMP model, i.e., Eq. (2). As She and Waymire [11] show, since Γ is constant, now the multiplier regains the infinite divisibility property for the third order velocity structure function S_3 but not for scales. Furthermore, $\Lambda^{M;D}=C(\ln S_3^M-\ln S_3^D)$, and so, by Eq. (8) and the definition of local scaling exponent in the beginning of Sec. II, we have $\lambda(t)=C\zeta_3^L(t)$ which shows that viscous (large-scale) effect squeezes (stretches) the "time" t resulting in acceleration of the defect speed with the transformation function $\zeta_3^L(t)$. Note that, for $F_\infty^{M;D}=(S_3^{M;D})^\Gamma$, the probability of the most intensive structure (MIS) is self-similar in the amplitude space with a single scaling exponent H whatever the scale is, as $p(W_{r^M r^D}^{\mathrm{MIS}})=[\|W_{r^M r^D}^{\mathrm{MIS}}\|=(S_3^{M;D})^\Gamma]^H$, the larger H is, the rarer is the MIS. This is the physical result of constant degree of intermittency quantified by β which is the meaning of ESS property in ESL.

2. Measurement, test, and digestion

Figures 6 and 7, called "ESS-EHS β-test" and "ESS-EHS Γ-C test," respectively, as in the captions, estimate the pa-

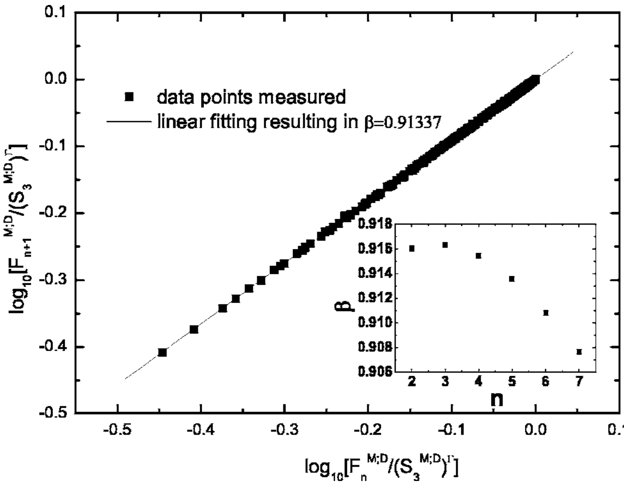

FIG. 6. ESS-EHS β-test, Eq. (14). The inset presents β fitted for different order n.

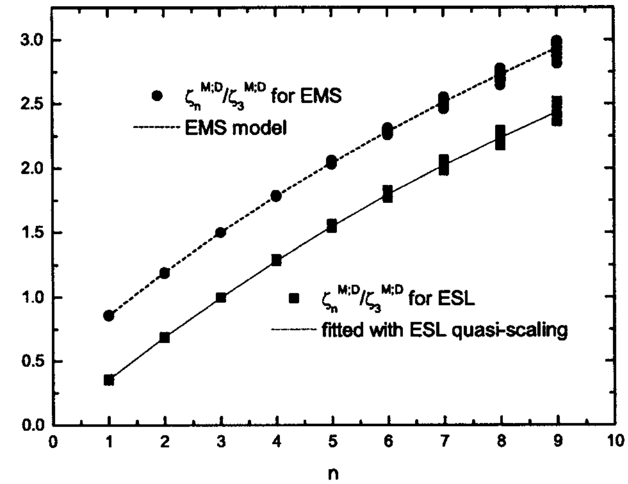

FIG. 8. Relative scaling exponents from quasiscaling exponents and fittings. Those for MS are shifted upward by 0.5. In measuring $\zeta_n^{M;D}/\zeta_3^{M;D}$, r^D, and r^M for ESL are those in Fig. 1 and Fig. 3 and those in Fig. 5 for EMS.

rameters by testing the structures of the claimed similarity Eq. (14) and exponent Eq. (15), resulting in the optimal $\Gamma=0.051$ and $\beta=0.913$; the fitted β for various n are also included in the inset showing very small variations. The optimal β is a little smaller than that by Ching *et al.* [16] and larger than that by Zou *et al.* [15]. Note that we have used ESS and making iterations in these two fittings to obtain values with least total errors, which is believed to produce more stable and reliable results. Figure 8 presents the fitting with ESS-ESL relative scaling exponents, the resulted parameters are included in Fig. 3 for comparison. We see that ESS-ESL works well, the ratios of quasiscaling exponents $\zeta_n^{M;D}/\zeta_3^{M;D}$ do collapse and the scatters, which are not monotonic with scales (for both cases) in Fig. 8 as we have observed in the data files (not shown here), so serves as error bars in the traditional linear fitting and the resulted parameters are stabilized (maybe rightly improved) much.

The ESS-ESL parameter Γ measured here is between the inertial saturation version of Chen and Cao [18] and the original one of She and Leveque [11]. If the latter parametrization is right, this should be explained as finite Reynolds number effects. When $\gamma(t)=0$, the local most intensive structure is shocklike [16,18]; our quasiscaling analysis now shows that this is an asymptotic state for $r\to\infty$ by the effect of large-scale stirring. We also cautiously comment that it seems quite unreasonable that the most intensive structures are still shocklike even when viscous effect enters.

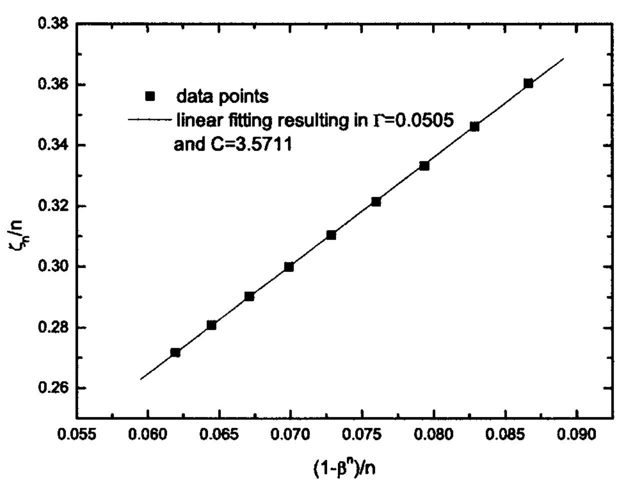

FIG. 7. ESS-EHS Γ-C test, Eq. (15). ζ_n is evaluated by averaging $\zeta_n^{M;D}/\zeta_3^{M;D}$ for distinct r^D.

B. ESS-EMS

1. Formulation

From Eq. (10) we have the EMS relative scaling exponent,

$$\zeta_n^{M;D}/\zeta_3^{M;D} = \frac{1-\log_2[(p^{M;D})^{n/3}+(q^{M;D})^{n/3}]}{1-\log_2(p^{M;D}+q^{M;D})}$$

$$=\zeta_n = 1-\log_2(\Pi^{n/3}+\tilde{\Pi}^{n/3}). \tag{16}$$

The $n\to\infty$ asymptotic relation being $p^{M;D}=(q^{M;D})^{\ln \Pi/\ln \tilde{\Pi}}$, not as ESS-ESL, Eq. (16) does not have a set of self-consistent relations (no such $p^{M;D}$, $q^{m;D}$, Π, and $\tilde{\Pi}$ satisfy it for all n) unless in the inertial range, i.e., ESS and EMS are not exactly consistent.

2. Measurement, test, and digestion

Since ESS and EMS are not consistent, we cannot apply ESS to fit the parameters as in ESS-ESL; however, we should see how severe it is. If the inconsistency is not so remarkable, the EMS phenomenology does accurately portray the physics and the quantification for nonconservative energy cascade is still reasonable. Figure 8 shows that EMS relative scaling with $\Pi=0.7$, $\tilde{\Pi}=1-\Pi$ fits well to the measurement. Numerical experiments presented in Fig. 9 show that the asymptotic relation $p^{M;D}=(q^{M;D})^{\ln \tilde{\Pi}/\ln \Pi}$ is "erroneous" while $p^{M;D}-q^{M;D}=0.4$ is quite accurate, ESS and EMS are approximately "consistent" with high accuracy in the ex-

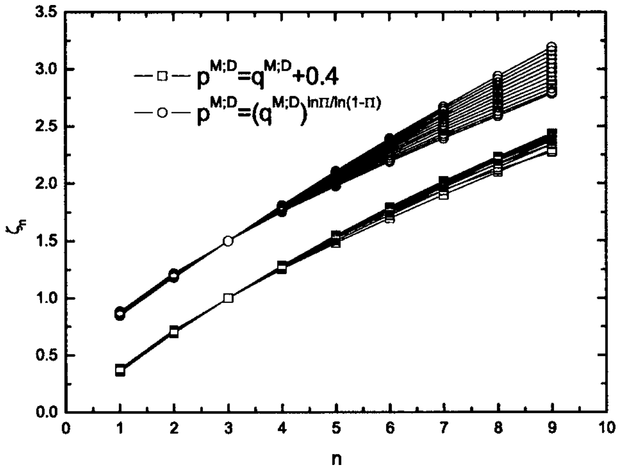

FIG. 9. Relative scaling exponents with the relation $p^{M;D}-q^{M;D}=0.4$ and the asymptotic relation $p^{M;D}=(q^{M;D})^{\ln \Pi/\ln \tilde{\Pi}}$ in Eq. (16) with $q^{M;D}$ ranging from 0.1 to 0.6 with step 0.04. Those of the latter are shifted upward by 0.5.

perimentally reachable range with $p^{M;D}-q^{M;D}\approx 0.4$ as presented in Fig. 5, showing nearly constant degree of intermittency, which is just the physical meaning of ESS property in EMS.

IV. SUMMARY AND DISCUSSION

We have shown that inertial theories of turbulence are useful for exploring the noninertial physics of turbulence. By performing quasiscaling analysis, we have successfully extended inertial phenomenologies to quantify the viscous and large-scale effects as case studies. The extension for SL model is consistent with ESS, while, except in the inertial range, that for MS model is not exactly so. However, within the present experimental resolution and capacity, either extended phenomenology is quite accurate, portraying respective physics, logarithmic-nonhomogeneous (nonstationary) Poissonian and nonconservative binomial cascade. Interestingly, while it is controvertible whether or not the correction to K41 is needed for the inertial turbulence [1,20], we here use the intermittency phenomenologies as finite Reynolds number theories. It is also possible that K41 normal scaling is the asymptotic state for $\beta^{M;D}\to 1$ in ESL or for $p^{M;D}-q^{M;D}\to 0$ in EMS which remains for further study.

Fluctuation amplitude PDFs, multifractal dimension spectrum and structure functions (of velocity increments) are all equivalent presentations of turbulence statistics. The present quasiscaling analysis for velocity structure functions indicate that EMS and ESL mechanism highly accurately reproduce the correct results for the intermediate ranges. Distinguishing the extrapolations for the statistics of very weak and intensive events concerns the neighborhood of zero points or the far tails of PDFs, the dimension spectrum at very large or small singularity exponent values, and moments for very low (even negative) or high orders; this is limited by the precision, measuring range of the instruments, sample size, and so on. This work is mainly based on measurements without much dynamical consideration, which will involve quantitatively those factors such as the viscosity, the characteristics of large-scale stirring and would lead to concrete models of $\lambda^{M;D}$ [or $\lambda(t)$] and $p^{M;D}$ in ESL and EMS. We note that a dynamical theory of multifractal may also be possible as was done very recently by Yakhot and Sreenivasan [21]. However, precise and massive experiments are highly desirable for further theoretical speculation and verification.

In the end, we remark that the RMP model, though not necessary, makes the formulation of quasiscaling theory transparent and suggestive and gives a clear physical picture. It bridges the PDFs of turbulent fluctuations at two distinct scales but, without an *ad hoc* ansatz of the "initial-time" PDF (i.e., the PDF at the largest scale studied), gives no information of the local PDF as was done recently by Beck *et al.* [22] in another line based on nonextensive statistical mechanics [8,9] which can also detect some scale-dependent information. Different approaches should be complementary and need further interaction towards an integrated theory of turbulence in the future.

ACKNOWLEDGMENTS

The author is grateful to the guidance and support of Professor Zhen-Su She. This work benefits from discussions with Professor Wei-Dong Su, Professor Yi-Peng Shi, and other LTCS members. The author also acknowledges the many interesting communications with Professor Jian Qian.

[1] U. Frisch, *Turbulence: The Legacy of A. N. Kolmogorov* (Cambridge University Press, Cambridge, England, 1995).
[2] R. H. Kraichnan, Proc. R. Soc. London, Ser. A **434**, 65 (1991).
[3] For example, those dealing with Kolmogorov equation, finite Reynolds number effects and finite size corrections, F. Moisy, P. Tabeling, and H. Willaime, Phys. Rev. Lett. **82**, 3994 (1999); J. Qian, Phys. Rev. E **60**, 3409 (1999); S. Grossmann, D. Lohse, V. L'vov, and I. Procaccia, Phys. Rev. Lett. **73**, 432 (1994).
[4] G. Paladin and A. Vulpiani, Phys. Rep. **156**, 147 (1987); K. R. Sreenivasan and C. Meneveau, Phys. Rev. A **38**, 6287 (1988); U. Frisch and M. Vergassola, Europhys. Lett. **14**, 439 (1991).
[5] R. Benzi, S. Ciliberto, R. Tripiccione, C. Baudet, F. Massaioli, and S. Succi, Phys. Rev. E **48**, R29 (1993).
[6] G. K. Batchelor, Proc. Cambridge Philos. Soc. **47**, 359 (1951); D. Lohse and A. Müller-Groeling, Phys. Rev. Lett. **74**, 1747 (1995); C. Meneveau, Phys. Rev. E **54**, 3657 (1996); S. Grossmann, D. Lohse, and A. Reeh, *ibid.* **56**, 5473 (1997); H. Fujisaka and S. Grossmann, *ibid.* **63**, 026305 (2001); S. Grossmann, D. Lohse, and A. Reeh, *ibid.* **61**, 5195 (2000).
[7] L. Chevillard, S. G. Roux, E. Leveque, N. Mordant, J.-F. Pinton, and A. Arneodo, Phys. Rev. Lett. **91**, 214502 (2003).

[8] C. Tsallis, J. Stat. Phys. **52**, 479 (1988).
[9] See, for example, the special issue of Physica D **193**, 1 (2004) containing selected contributions from an international workshop on “Anomalous Distributions, Nonlinear Dynamics, and Nonextensivity,” held in Santa Fe, New Mexico, 6C9 November 2002.
[10] T. Gotoh and R. H. Kraichnan, Physica D **193**, 231 (2004).
[11] Z. S. She and E. Leveque, Phys. Rev. Lett. **72**, 336 (1994); B. Dubrulle, *ibid.* **73**, 959 (1994); Z.-S. She and E. C. Waymire, *ibid.* **74**, 262 (1995).
[12] C. Meneveau and K. R. Sreenivasan, Phys. Rev. Lett. **59**, 1424 (1987); J. Fluid Mech. **224**, 429 (1991).
[13] Nonhomogeneous Poisson process is a model for nonstationary arrival process and is widely used in areas such as reliability theory, see for example, E. Çinlar, *Introduction to Stochastic Processes* (Prentice Hall, Englewood Cliffs, NJ, 1975). The key idea is to generalize the constant arrival rate λ of Poisson process to be time dependent $\lambda(t)$.
[14] R. Benzi, L. Biferale, S. Ciliberto, M. V. Struglia, and R. Tripiccione, Physica D **96**, 162 (1996).
[15] Z. Zou, Y. Zhu, M. Zhou, and Zhen-Su She, Fluid Dyn. Res. **33**, 493 (2003).
[16] E. S. C. Ching, Z.-S. She, W. Su, and Z. Zou, Phys. Rev. E **65**, 066303 (2002).
[17] The phenomenologies presented in this work do not distinguish between velocity increment and its absolute value; for the same consideration of statistical stability as in other works [5,15,16], we compute the velocity structure function by the absolute value.
[18] E. A. Novikov, Phys. Rev. E **50**, R3303 (1994); M. Nelkin, *ibid.* **52**, R4610 (1995); S. Chen and N. Cao, *ibid.* **52**, R5757 (1995).
[19] E. Leveque and C. R. Koudella, Phys. Rev. Lett. **86**, 4033 (2001).
[20] J. Qian, Phys. Rev. E **58**, 7325 (1998); T. S. Lundgren, Phys. Fluids **15**, 1074 (2003).
[21] V. Yakhot and K. R. Sreenivasan, Physica A **343**, 147 (2004).
[22] C. Beck, G. S. Lewis, and H. L. Swinney, Phys. Rev. E **63**, 035303(R) (2001).